MECHANISTICAL STUDIES ON THE PRODUCTION OF FORMAMIDE (H₂NCHO) WITHIN INTERSTELLAR ICE ANALOGS

Brant M. Jones[1,2], Christopher J. Bennett[1,2], and Ralf I. Kaiser[1,2,3]
[1] Department of Chemistry, University of Hawai'i at Manoa, Honolulu, HI 96822, USA; ralfk@hawaii.edu
[2] NASA Astrobiology Institute, University of Hawai'i at Manoa, Honolulu, HI 96822, USA

ABSTRACT

Formamide, H_2NCHO, represents the simplest molecule containing the peptide bond. Consequently, the formamide molecule is of high interest as it is considered an important precursor in the abiotic synthesis of amino acids, and thus significant to further prebiotic chemistry, in more suitable environments. Previous experiments have demonstrated that formamide is formed under extreme conditions similar throughout the interstellar medium via photolysis and the energetic processing of ultracold interstellar and solar system ices with high-energy protons; however, no clear reaction mechanism has been identified. Utilizing a laboratory apparatus capable of simulating the effects of galactic cosmic radiation on ultralow temperature ice mixtures, we have examined the formation of formamide starting from a variety of carbon monoxide (CO) to ammonia (NH_3) ices of varying composition. Our results suggest that the primary reaction step leading to the production of formamide in low-temperature ices involves the cleavage of the nitrogen–hydrogen bond of ammonia forming the amino radical (NH_2) and atomic hydrogen (H), the latter of which containing excess kinetic energy. These suprathermal hydrogen atoms can then add to the carbon–oxygen triple bond of the carbon monoxide (CO) molecule, overcoming the entrance barrier, and ultimately producing the formyl radical (HCO). From here, the formyl radical may combine without an entrance barrier with the neighboring amino radical if the proper geometry for these two species exists within the matrix cage.

Key words: astrochemistry – cosmic rays – ISM: clouds

Online-only material: color figures

1. INTRODUCTION

The simplest molecule containing the biologically crucial peptide bond [–(O)C–N(H)–] is formamide (H_2NCHO). Due to the functionality of the peptide bond, this molecule has gained significant attention throughout the years as it has been proposed to be a possible precursor in the abiotic synthesis of more complex molecules under prebiotic conditions (Brucato et al. 2006b; Saladino et al. 2009, 2007, 2005, 2003, 2001; Senanayake & Idriss 2006). Experiments have demonstrated that amino acids and complex carbon, hydrogen, oxygen, and nitrogen-bearing (CHON) organics can be produced starting simply with formamide (Apene & Mikstais 1978; Boden & Back 1970; Costanzo et al. 2007; Dederichs et al. 1975; Ivanov & Vladovska 1978; Kostakis et al. 2007). From here a condensation reaction between these amino acids in the presence of a mineral catalysis may take place leading to the formation of polypeptides and/or simple proteins (Bujdák & Rode 1999; Lambert 2008; Lambert et al. 2009; Rimola et al. 2006). An excellent review by Saladino et al. articulates well how formamide may provide all the components necessary for the formation of nucleic polymers under prebiotic or abiotic conditions (Saladino et al. 2007), including the formation of acyclonucleosides which may solve the problem of poor reactivity between nucleic bases and ribose (Saladino et al. 2009). If one is to except the notion that formamide is an important precursor to biologically important molecules then the questions arise as to where and how formamide was synthesized in extraterrestrial environments.

Gas-phase formamide has been detected within the interstellar medium toward Sgr B2 with a derived upper limit on the column density of 2.2×10^{16} cm^{-2} and a rather conservative lower limit estimate of 4×10^{11} cm^{-2} (Rubin et al. 1971). A more recent observation toward Sgr B2(N) revealed two new transitions of formamide ($3_{12}-3_{13}$, $1_{01}-1_{00}$) allowing for a more accurate determination of the column densities, yielding an upper limit of $5.86 \pm 0.12 \times 10^{14}$ cm^{-2} and a lower limit of $1.13 \pm 0.30 \times 10^{14}$ cm^{-2} (Hollis et al. 2006). The column densities of formamide are on the order of 10^{10} less than the molecular hydrogen column densities, $n(H_2) \sim 10^{24}$ cm^{-2} (Scoville et al. 1975). It should be noted that the authors of the original study identifying formamide in Sgr B2 did not find any evidence of this particular molecule in W3 (continuum), W3(OH), Ori A, Ori B, the dust cloud L134, W49, W51, or DR 21 (Rubin et al. 1971). In addition to the gas-phase formamide detected toward the hot core of Sgr B2, a survey of the molecules out-gassing from the nuclei of comet C/1995 O1 (more commonly referred to as Hale–Bopp) has revealed the presence of formamide with an abundance of 0.01%–0.02% relative to water and a production rate ranging from 9 to 23×10^{26} molecules per second. An assumption was made that formamide, as well as the other species observed, was released from the nucleus of the comet via sublimation (Bockelée-Morvan et al. 2000). Formamide has also been tentatively assigned within the solid phase on icy grains toward the protostellar objects NGC 7538 IRS9 and W33A. The assignment was based on a simple qualitative comparison of laboratory spectra of solid isocyanic acid (HNCO) held at 10 K upon being subjected to vacuum ultraviolet (VUV) photolysis with that of *ISO*–SWS spectra (Raunier et al. 2004) and to the laboratory spectra of an assortment of matrix-isolated organics (Schutte et al. 1999). Unfortunately, quantifying the amount of formamide present within these cold objects is difficult due to the broad overlapping features with, for instance, ammonia. Consequently, the amount of solid formamide believed to be

---

present within these young protostellar objects is unknown. To date, only thrice has formamide *definitively* been identified within the interstellar medium, twice within the molecular cloud Sgr B2 (N) and once in the coma surrounding comet Hale–Bopp. Accordingly, very little is known about the distribution of formamide throughout the interstellar medium.

Several reaction pathways have been previously proposed that may lead to formamide starting from a binary mixture of ammonia and carbon monoxide in the solid state (Grim et al. 1989; Hagen 1982) and gas phase (Hubbard et al. 1975). These pathways are summarized as follows, where the electronic term symbols have been omitted for clarity:

$$NH_3 + CO \rightarrow H_2NCHO \quad (1)$$

$$NH_3 \rightarrow NH_2 + H \quad (2a)$$

$$NH_2 + CO \rightarrow H_2NCO \quad (2b)$$

$$H_2NCO + H \rightarrow H_2NCHO \quad (2c)$$

$$2H_2NCO \rightarrow H_2NCHO + HNCO \quad (2d)$$

$$NH_3 \rightarrow NH_2 + H \quad (3a)$$

$$H + CO \rightarrow HCO \quad (3b)$$

$$HCO + NH_2 \rightarrow H_2NCHO. \quad (3c)$$
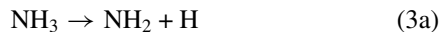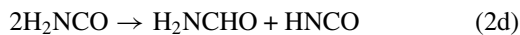
Reaction pathway (1) maybe discounted immediately as both carbon monoxide and ammonia are closed-shell species and as a result, this reaction has a significantly large entrance barrier for the reaction as shown experimentally and theoretically (Kakumoto et al. 1985; Nguyen et al. 2011). Recent quantum-mechanical calculations done by Nguyen et al. on the decomposition pathways of formamide show that the products CO and NH_3 require an activation energy of 336 kJ mol^{-1} with the overall enthalpy being 26 kJ mol^{-1} above the ground state of formamide. If we consider the reverse reaction, $CO + NH_3 \rightarrow H_2NCHO$, this value corresponds well to the reaction exogercity as derived from the National Institute of Standards and Technology (NIST) database of 29 kJ mol^{-1} (Afeefy et al. 2010). From this, we may conclude that the energy barrier necessary for reaction scheme (1) is on the order of 310 kJ mol^{-1}. Reaction scheme (2c) however involves the reaction of atomic hydrogen with the H_2NCO radical, which has been shown to predominantly form isocyanic acid (HNCO) in the low-pressure (<10 torr) limit (Woolley & Back 1968); consequently, this pathway may be insignificant in the gas-phase photolysis of a low-density carbon monoxide–ammonia mixture in conditions such as those of a cold molecular cloud. The authors also noted that within the high-pressure limit (10–23 torr), a residue was formed on the surface of the glass thought to be caused by subsidiary reactions and consequently the evolution of larger organic molecules such as urea and biuret, correlating well with past observations of ammonia–carbon monoxide chemistry under energetic processing in a significantly dense state i.e., high-pressure gas and solid phase (Agarwal et al. 1985; Grim et al. 1989; Hubbard et al. 1975; Raunier et al. 2004).

A study on the VUV photolysis of solid isocyanic (HNCO) acid held at 10 K (Raunier et al. 2004) also identified formamide as one of the products formed. The authors proposed the photodissociation of HNCO to be the primary source of atomic hydrogen. From here, the hydrogen atom may sequentially add to HNCO via a two-step addition,

$$H + HNCO \rightarrow H_2NCO \quad (4a)$$

$$H + H_2NCO \rightarrow H_2NCHO, \quad (4b)$$

to ultimately form H_2NCHO. Thus, this experiment would elucidate that in the event of producing HNCO in significant quantities from the disproportionation of the NH_2CO radical (scheme (2d)), further energetic processing of isocyanic acid may still lead to the production of formamide. Contrary to the above, however, is that HNCO will react quite rapidly with NH_3 to form ammonium cyanate ($NH_4^+OCN^-$) even at temperatures as low as 10 K as demonstrated experimentally (Raunier et al. 2004, 2003). Accordingly, the reaction pathway involving isocyanic acid leading to formamide via the sequential addition of atomic hydrogen may be discounted based on the observation that in the presence of ammonia, HNCO will preferentially react immediately with ammonia, forming ammonium cyanate.

Of the above-mentioned pathways, most ultimately start with the production of a hydrogen atom. Both of the reactions have been shown theoretically to have an entrance barrier, i.e., the minimum energy required for the reaction to initiate. Typically, for a molecular cloud, these energy barriers are significantly higher than the available kinetic energy of the molecules even for a "hot" molecular core such as Sgr B2 (M) with temperatures reaching ∼300 K. Similarly, density is also an important parameter to consider as it directly affects the number of collisions per unit time. Both of the suggested plausible reaction schemes ((2) and (3)) listed above involve a three-step process which physically requires a third body collision in the gas phase. For a typical cold molecular cloud with a number density of 10^2–10^4 cm^{-3}, a collision of this nature would occur once in every few 10^9 years, and hence inconsequential compared to the average lifetime of 10^5–10^6 yr (Kaiser 2002). As such, one may suspect the energetic processing of ices leading to the formation of more complex CHON species such as formamide as the primary means of synthesis before being released into the gas phase either through sublimation or grain–grain collisions.

Several studies have identified the production of formamide starting from the energetic processing of a simple binary mixture containing carbon monoxide and ammonia (Demyk et al. 1998; Ferris et al. 1974; Grim et al. 1989; Hagen 1982; Hudson & Moore 2000; Milligan & Jacox 1965) under conditions relevant to the interstellar medium. However, thus far only speculation as to what the actual reaction pathway is has been proposed (reaction schemes above). The first study identifying the formation of formamide was that done by Hubbard et al. in the gas phase, of which the primary product observed in the ultraviolet photolysis of a binary gas-phase CO–NH$_3$ mixture was ammonium cyanate ($NH_4^+OCN^-$) with small amounts of urea, biurea, biuret semi-carbazide, formamide, and cyanide being observed (Hubbard et al. 1975). The authors proposed that the production of formamide appeared to be from one of the two possible reaction pathways, these being the combination of atomic hydrogen with NH_2CO (reaction scheme (2c)) or the disproportionation of NH_2CO (reaction scheme (2d)) forming the products formamide and isocyanic

Table 1
Corresponding Partial Pressures of CO:NH$_3$ Premixed in the Gas Mixing Chamber Before Expansion Yielding the Corresponding Desired Ratio (Left Column)
Based Upon the Derived Column Densities (molecules cm^{-2}) of Carbon Monoxide and Ammonia

Ice Ratio (CO:NH$_3$) $\pm 1.4\%$	Partial Pressure of CO (mbar) ± 1 mbar	Partial Pressure of NH$_3$ (mbar) ± 1 mbar
11:2	700	70
5:2	675	135
2:5	400	400
1:10	114	686
1:20	62	738

acid. As mentioned earlier, the reaction of atomic hydrogen with NH$_2$CO was deemed less likely to occur based on a previous study (Woolley & Back 1968) showing that the primary product of the reaction between these two to be isocyanic acid (HNCO) and thus proposed the reaction to be inconsequential. The authors of this study also recognized the possibility of reaction scheme (1); however, we discounted this route based upon the energetics of breaking the NH (435 kJ mol^{-1}) bond in ammonia in comparison to forming the C–H bond (300 kJ mol^{-1}) in formamide.

Of the experiments involving the energetic processing of CO–NH$_3$ ices mentioned above (Demyk et al. 1998; Grim et al. 1989; Hagen 1982; Hudson & Moore 2000), Hagen proposed several possible reaction pathways leading to the formation of formamide. However, as pointed out by Grim et al., some of the assignments originally made by Hagen were incorrect and required further revision. The uncertainty of Hagen's assignment was based upon the discrepancies between the matrix-isolated formamide and that of pure formamide; however, these were largely due to hydrogen bond formation (King 1971). Additionally, as was also pointed out in a study by Hudson and Moore focusing on the production of OCN$^-$ within interstellar grains, further experiments were needed to test the proposed reaction pathways leading to the synthesis of formamide (Hudson & Moore 2000). Similarly, previous studies have also noted the production of formamide under the irradiation of CO–NH$_3$ ices (Demyk et al. 1998; Ferris et al. 1974; Milligan & Jacox 1965). However, as the production of formamide was not the main intention of the investigation, no detailed discussion of the production pathway(s) of formamide was/were made.

The goal of the present experiments is to determine the reaction pathway(s) leading to the production of formamide under conditions similar to the energetic processing of cold interstellar grains induced via background galactic cosmic rays through laboratory simulation of this environment.

2. EXPERIMENTAL DETAILS

The experiments were carried out in a contamination-free ultrahigh vacuum stainless steel chamber (Bennett et al. 2004). This vessel is evacuated down to a base pressure typically to the order of 5×10^{-11} torr using oil-free magnetically suspended turbomolecular pumps. A closed-cycle helium refrigerator cools a highly polished silver mirror to 11.7 ± 0.3 K; the latter is held in the center of the chamber and is freely rotatable within the horizontal center plane of the chamber. A binary mixture of ammonia (99.99%; Matheson Gas Products, Inc.) and carbon monoxide (99.99%; The Specialty Gas Group) was prepared in a separate gas mixing vessel (Table 1). The gas mixture was then deposited through a glass capillary array held at a distance of 5 mm from the silver target for 40 minutes

with a background pressure in the main chamber of 2.5×10^{-8} torr. A Fourier infrared transform spectrometer (Nicolet 6700) monitored the samples throughout the duration of the experiment with an IR spectrum collected every 2 minutes in the range of 6000–400 cm^{-1} at a resolution of 4 cm^{-1}. A quadrupole mass spectrometer (Balzer QMG 420) operating in residual-gas analyzer mode with an electron impact ionization energy of 100 eV allows for the detection of species in the gas phase for the duration of the experiment.

Column densities of the reactants and products were calculated via a modified Beers–Lambert law (Bennett et al. 2004). The average column density of carbon monoxide was derived from the v_1 band at 2136 cm^{-1}, the ^{13}CO v_1 band at 2091 cm^{-1}, and the $2v_1$ overtone band at 4251 cm^{-1} using the absorption coefficients as determined from (Gerakines et al. 1995) as listed in Table 2. The average column density of ammonia was determined from v_2 at the ~1070 cm^{-1} band and the broadband (ranging from 3200 to 3500 cm^{-1} due to various dimers, trimers, and aggregates formed) using absorption coefficients as determined by d'Hendecourt & Allamandola (1986) as listed in Table 2. The density of carbon monoxide was taken to be 1.03 g cm^{-3} (Krupskii et al. 1973) while 0.86 g cm^{-3} was used for the density of ammonia (Romanescu et al. 2010). Based upon these densities, the average thicknesses of the ice samples were determined to be 150 ± 30 nm with ratios of the column densities as compiled in Table 1.

In our experiments the ices are energetically processed through bombardment with 5 keV electrons. The Galactic cosmic-ray field consists predominantly of protons, which have a distribution maximum of a few 10 MeV and lose about 99.99% of their kinetic energy via transfer of their kinetic energy to the electronic system of the target molecules (here carbon monoxide and ammonia). This electronic energy transfer generates energetic electrons with energies up to a few keV; in addition, dynamic simulations of the ice mixtures using the CASINO code (Hovington et al. 1997) determined the electronic linear energy transfer (LET) ranging from 3.8 to 4.1 keV μm^{-1} suggesting that the torrent of MeV protons striking the ice target within the interstellar medium holds a similar value as the 5 keV electrons used in the present experiments, i.e., a few keV μm^{-1} (Bennett et al. 2004; Johnson 1990). Therefore, our laboratory experiments mimic the formation of formamide in carbon monoxide–ammonia solid state complexes via charged particles through electronic energy-loss processes in interstellar ices as condensed on grains in molecular clouds at 10 K. From this point, formamide may proceed into the gas phase via grain–grain collisions (Markwick et al. 2000), shocking of the interstellar medium (Flower & Pineau des Forets 1994) or once the cold cloud proceeds through a hot molecular core stage, where the elevated temperatures can cause the newly formed formamide molecules to sublime, upon which are detected in the gas phase via radio telescopes.

Table 2
Identified Peaks of the Pristine Ices at 12 K

Molecular Species	Vibrational Mode	Observed Band Position (cm^{-1})					Literature Value (cm^{-1})	Absorption Value (×10^{-17} cm mol^{-1})
		11 CO:2 NH$_3$	5 CO:2 NH$_3$	2 CO:5 NH$_3$	10 NH$_3$:1 CO	20 NH$_3$:1 CO		
NH$_3$	v_2	983 1006	1053	1078	1059 1107	1066 1113	1070[1], 1097[2], 1060[3]	1.7[1]
NH$_3$	v_4	1628	1628	1628	1631	1629	1628[2], 1624[1]	...
NH$_3$	NH$_3$ aggregate[4]	1641	1649	...	...	...	1647[4]	...
NH$_3$	$v_2 + v_L$	...	...	...	1875	1880	1876[2]	...
^{13}C^{18}O	v_1	2046	2044	2044	...	...	2041[5]	...
^{13}CO	v_1	2090	2090	2090	2090	...	2091[6,7]	1.3[7]
CO	v_1	2136	2135	2134	2136	2136	2136[6,7]	1.1[7]
(NH$_3$:CO) complex	?	2139	2142	2142	...	...	2142[8]	...
CO	$v_1 + v_L$	2208	2194	2191	...	...	2208[6]	...
NH$_3$	v_1 v_2 v_3 ($v_1 + v_L$)	3200–3500	3200–3500	3200–3500	3200–3500	3200–3500	3212[2] 3290[2] 3372[2] 3472[2]	1.1[1]
CO	$2v_1$	4252	4250	4250	...	...	4251[6,7]	0.016[7]
NH$_3$	$(v_1 + v_2)^2$				4340	4347	4345[2]	...
NH$_3$	$(v_3 + v_2)^2$ $(v_1 + v_2)^9$	4441	4460	4468	4476	4477	4478[2] 4474[9]	0.087 ± 0.003[9]
NH$_3$	$(v_1 + v_4)$?	5027	5023	5004	4995	5994	4993[9]	0.081 ± 0.003[9]

References. (1) d'Hendecourt & Allamandola 1986; (2) Zheng & Kaiser 2007; (3) Jacox & Milligan 1963; (4) Suzer & Andrews 1987; (5) Bennett et al. 2010; (6) Jamieson et al. 2006; (7) Gerakines et al. 1995; (8) Bennett et al. 2010; (9) Gerakines et al. 2005; (10) Hagen 1982; (11) Grim et al. 1989; (12) Minkwitz 1975; (13) Brucato et al. 2006a; (14) Brucato et al. 2006b; (15) Hudson & Moore 2000; (16) Raunier et al. 2003; (17) Forney et al. 2003; (18) Bennett & Kaiser 2007; (19) Bennett et al. 2005; (20) Demyk et al. 1998; (21) Broekhuizen et al. 2004; (22) Kim et al. 1998; (23) Gerakines et al. 2001; (24) Yamada & Person 1964; (25) Hudgins et al. 1993; (26) Zheng et al. 2008; (27) Sylwester & Dervan 1984; (28) King 1971; (29) Harvey & Ogilvie 1962.

The carbon monoxide–ammonia ice matrices were irradiated isothermally at 11.7 ± 0.3 K with 5 keV electrons generated with an electron source (Specs EQ 22/35) at a beam current of 100 nA for 1 hr by scanning the electron beam over an area of 3.2 ± 0.3 cm^2. Assuming an extraction efficiency of 78.8% as stated by the manufacture, the sample was exposed to a total of 1.8×10^{15} electrons during irradiation. After scaling for the difference in the electronic LET in our experiments (3.8–4.1 keV μm^{-1}) to the actual cosmic-ray energy deposition of a 10 MeV proton determined to be an average of 4.23 keV μm^{-1} (Kaiser & Roessler 1998), we can conclude that 1 s of our laboratory experiments simulates a processing of interstellar ices over $1.5 \pm 0.3 \times 10^{10}$ s. Therefore, our laboratory experiments mimic a timescale of $1.7 \pm 0.3 \times 10^6$ yr which is on the order of a typical lifetime of an interstellar cloud (Kaiser 2002). Upon completion of irradiating the sample with electrons, the ice matrix was undisturbed for 1 hr at which point heating to a final temperature of 300 K at a rate of 0.5 K minute^{-1} began.

3. RESULTS

3.1. Infrared Band Assignments

Band positions of the pristine ice samples as shown in Figure 1 (left-hand column, black lines) are summarized in Table 2. Upon irradiation with the energetic electrons at 0.1 μA for 1 hr, new absorption bands are observed in the IR as shown in Figure 1 (left-hand column, red lines). The new species identified in the entire range of the FTIR (6000–400 cm^{-1}) are listed in Table 3. Although time has been taken to ensure a thorough assignment of the peaks observed in the infrared spectrum, this report will focus only on the species relevant to the formation of formamide and its precursors. Consequently, we have focused on a "region of interest" in the vicinity of 1800–1300 cm^{-1}. The molecular species associated within this region of interest have been identified at 50 K and 150 K; see Tables 4 and 5, respectively. In each of the irradiated CO:NH$_3$ ice matrices, a residue was observed in the IR with the band positions of the observed peaks along with a tentative assignment on the vibrational characterization given in Table 6.

Formamide was identified via several different vibrational modes as outlined in Table 2. The v_6 (CH scissoring) mode at 1389 cm^{-1} was consistently witnessed for each of the ratios irradiated during the experiment and isolated well enough such that the temporal profile could be determined without using a Gaussian deconvolution technique. This peak as well as others agrees well with previous assignments as reflected in Tables 3–5. The formyl (HCO) radical was identified via v_3 (CO stretching) at 1857 cm^{-1} for 11:2 irradiate ice sample and at 1852 cm^{-1} for the 5:2 ice matrix. This assignment is
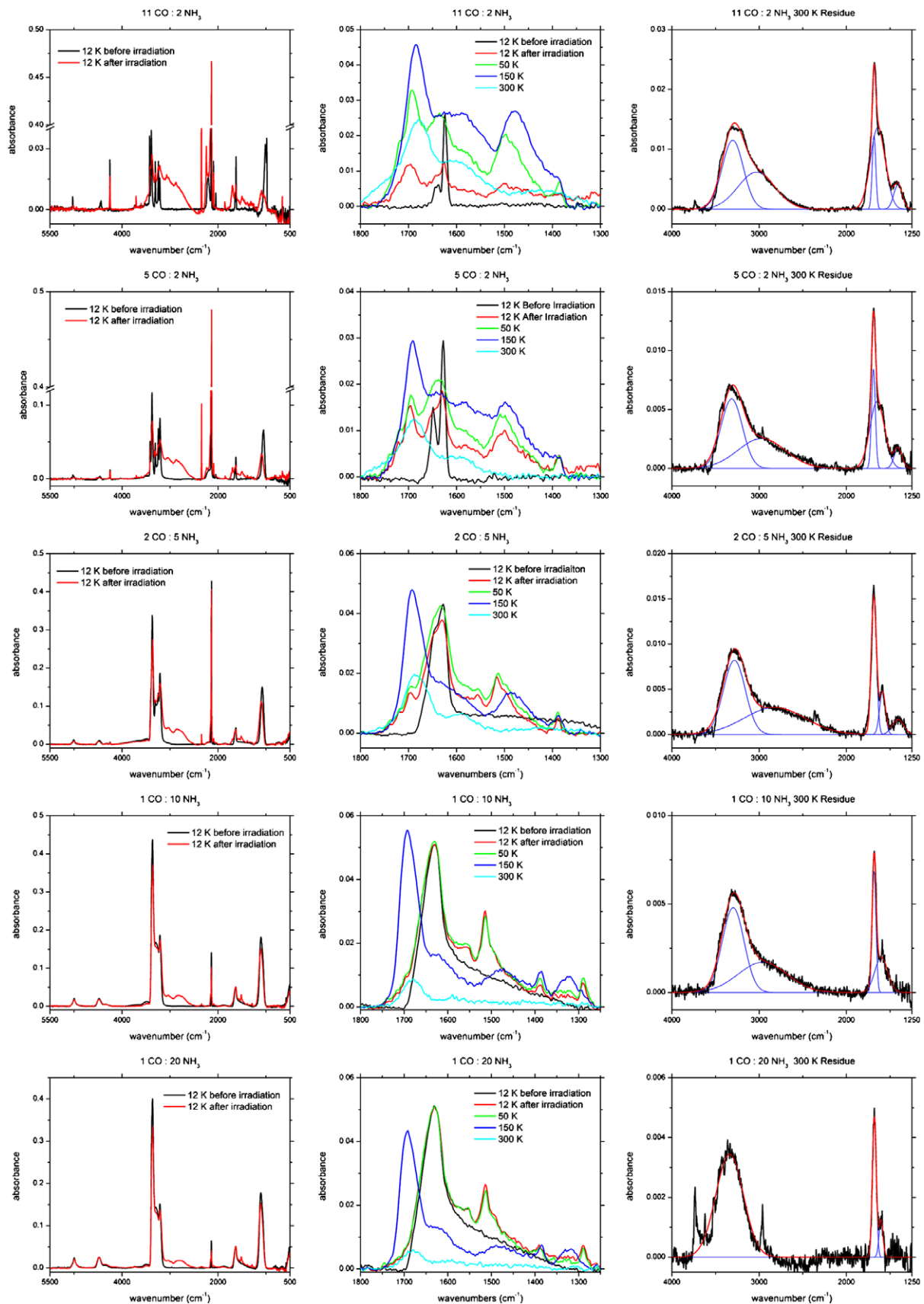
Figure 1. Infrared spectra of the pristine (black) and irradiated ices (red) in the wavenumber range of 5500–500 cm^{-1} (far left). The middle column shows the IR spectra of the pristine and irradiate ices at 12 (red), 50 (green), 150 (blue), and 300 K (cyan) in the wavenumber range of 1800–1300 cm^{-1} designated in the main body text as the region of interest with respect to formamide. The far right hand of the figure displays the deconvoluted IR spectra of the residue formed upon warming the irradiated ice mixtures to 300 K. For a tentative characterization of these bands, please see Table 5. The figure is oriented such that the respective concentration of carbon monoxide decreases from top to bottom.

(A color version of this figure is available in the online journal.)

Table 3
Identified Peaks of the Irradiate Ices at 12 K

Molecular Species	Vibrational Mode	Observed Band Position (cm^{-1})					Literature Value (cm^{-1})	Absorption Value ($\times 10^{-17}$ cm mol^{-1})
		11 CO:2 NH_3	5 CO:2 NH_3	2 CO:5 NH_3	10 NH_3:1 CO	20 NH_3:1 CO		
CO_2	v_2	660	. . .	. . .	. . .	. . .	666[6]	0.54[6]
cis N_2H_2	v_4	. . .	. . .	. . .	1290	1290	1290[10] 1300[11] 1286[12]	. . .
H_2NCHO	v_7	1315	1322	. . .	. . .	. . .	1328[11,13,14]	0.85[13]
H_2NCHO	v_6	1388	1389	1389	1387	1390	1388[10,11,13]	0.68[13]
NH_4^+	v_4	1500	1499	1516	1514	1514	1499[10,15] 1495[16] 1478[13]	. . .
$H_2NCO_2^-$		. . .	. . .	1556	1556	1552	1553[11]	. . .
H_2NCHO	v_4	1700	1697	1695	1697	. . .	1699[11] 1708[13,14]	6.54 ($v_4 + v_5$)[13]
H_2CO		. . .	. . .	1740	. . .	. . .	1736[11]	
HOCO	v_2	1841	1837	1840	. . .	. . .	1846[17]	3.6[18]
HCO	v_3	1857	1851	. . .	. . .	. . .	1853[19] 1854[11]	1.5[19]
OCN^-	v_3	2157	2160	2154	2154	2154	2160[8,11,15,20,21]	13[21]
C_3O_2	v_1	2192	. . .	. . .	. . .	. . .	2194[6]	. . .
C_3O_2	v_3	2242	. . .	. . .	. . .	. . .	2242[6]	47[6] 36[22] 1.3[23]
$^{13}CO_2$	v_3	2279	. . .	. . .	. . .	. . .	2281[6]	7.8[7]
CO_2	v_3	2343	2343	2343	2342	. . .	2346[6]	7.6[24] 10[6] 14[25]
C_3O_2	($v_2 + v_4$)	2399	. . .	. . .	. . .	. . .	2399[6]	0.8[23]
N=NH_2	v_5	. . .	2810	2802	2805	2805	2805[26,27]	. . .
?		2873	2860	2867	. . .	. . .	. . .	. . .
cis HNNH	v_1	3045	3050	3053	3040	3035	3052[26]	. . .
CO_2	($2v_2 + v_3$)	3600	3598	. . .	. . .	. . .	3602[6]	0.14[7], 0.26[25]
CO_2	($v_1 + v_3$)	3706	3702	. . .	. . .	. . .	3707[6]	. . .

Note. See footnotes to Table 2.

consistent with the previously reported matrix-isolated values of 1856 and 1858 cm^{-1} in xenon (Maier & Lautz 1998; Pettersson et al. 1999), 1863 cm^{-1} in argon (Milligan & Jacox 1969), 1861 cm^{-1} in carbon monoxide (Ewing et al. 1960), and 1853 cm^{-1} for a 1:1 ratio of carbon monoxide to methane irradiated ice (Bennett et al. 2005). For the same ratio of ices where the HCO band was identified, a shoulder consisting of ∼1840 cm^{-1} was observed. This peak position was previously assigned to the NCO stretching of the carbamyl NH_2CO radical (Grim et al. 1989; Hagen 1982). However, a more recent infrared study on this particular radical has experimentally identified the vibrational modes, providing evidence that this assignment may be incorrect (Pettersson et al. 1999). The experimentally observed band position for the NCO stretching vibrational mode ranged from 1794 to 1812 cm^{-1}. This is in addition to previous experiments identifying hydrocarboxyl (HOCO) radical at ∼1840 cm^{-1}; we have accordingly assigned the

observed shoulder at this frequency to the hydrocarboxyl radical in agreement with previous matrix-isolation studies; 1848 cm^{-1} in neon (Forney et al. 2003), 1844 cm^{-1} in argon (Jacox 1988), 1833 cm^{-1} in carbon monoxide (Milligan & Jacox 1971), and 1847 cm^{-1} in a 1:1 ratio of carbon dioxide to methane irradiated ice (Bennett & Kaiser 2007).

In order to examine all of the possible routes pertaining to the formation of formamide upon irradiation of a binary mixture of carbon monoxide and ammonia, isocyanic acid (HNCO) was searched for based upon IR bands identified in the matrix-isolation study of HNCO (Pettersson et al. 1999). Pettersson et al. identified several strong bands including the v_1 (NH stretch) at ∼3500 cm^{-1}, v_2 (NCO asymmetric stretching) at ∼2250 cm^{-1}, v_4 (HNC, CNO bending) at ∼760 cm^{-1}, and v_5 (HNC, CNO bending) at ∼570 cm^{-1} (note that approximate values are stated in this paper simply as a reference point—the original study identified these peaks with far more accuracy;

Table 4
Identified Peaks of the Irradiate Ices at 50 K After the Sublimation of CO Within the Region of Interest (1800–1300 cm^{-1})

Molecular Species	Vibrational Mode	Observed Band Position (cm^{-1})					Literature Value (cm^{-1})	Absorption Value ($\times 10^{-17}$ cm mol^{-1})
		11 CO:2 NH$_3$	5 CO:2 NH$_3$	2 CO:5 NH$_3$	10 NH$_3$:1 CO	20 NH$_3$:1 CO		
cis N$_2$H$_2$	. . .	. . .	. . .	. . .	1290	1290	1290[10] 1300[11] 1286[12]	. . .
H$_2$NCHO	v_6	1386	1389	1389	1388	1390	1388[10,11,13]	0.68[13]
NH$_4$$^+$	v_4	1500	1507	1514	1514	1514	1499[10,15] 1495[16] 1478[13]	. . .
H$_2$NCO$_2$$^-$ (?)		. . .	. . .	1556	1554	1553	1553[11]	. . .
R–NH$_2$	δ_{NH_2}	1583	1581	. . .	. . .	. . .	1590[28]	. . .
H$_2$NCHO	v_5	1637	1637	. . .	. . .	. . .	1631[13]	. . .
H$_2$NCHO	v_4	1696	1695	1692	. . .	. . .	1699[11] 1708[13]	6.54 ($v_4 + v_5$)[13]
H$_2$NCHO	v_4	1720	1720	1718	. . .	. . .	1724[11]	. . .
H$_2$CO	v_2	. . .	1740	1740	. . .	. . .	1736[11] 1742[29]	. . .

Note. See footnotes to Table 2.

Table 5
Identified Peaks of Irradiate Ice at 150 K After the Sublimation of NH$_3$ Within the Region of Interest (1800–1300 cm^{-1})

Molecular Species	Vibrational Mode	Observed Band Position (cm^{-1})					Literature Value (cm^{-1})	Absorption Value ($\times 10^{-17}$ cm mol^{-1})
		11 CO:2 NH$_3$	5 CO:2 NH$_3$	2 CO:5 NH$_3$	10 NH$_3$:1 CO	20 NH$_3$:1 CO		
H$_2$NCHO					1323	1321	1327[11] 1328[13]	0.85[13]
H$_2$NCHO	v_6	1389	1389	1389	1387	1386	1388[10,11,13]	0.68[13]
NH$_4$$^+$	v_4	1479	1480	1484	1474	1479	1499[10,15] 1495[16] 1478[13]	. . .
R–NH$_2$	δ_{NH_2}	1590	1590	1600	. . .	. . .	1590[28]	. . .
H$_2$NCHO	v_4	1684	1697	1696	1694	1692	1699[11] 1708[13]	6.54 ($v_4 + v_5$)[13]

Note. See footnotes to Table 2.

Table 6
Identified Peaks and their Suggestive Band Characterization of the Residue Formed from the Irradiated Ice at 300 K

Characterization	Observed Band Position (cm^{-1})					Literature Value (cm^{-1})
	11 CO:2 NH$_3$	5 CO:2 NH$_3$	2 CO:5 NH$_3$	10 NH$_3$:1 CO	20 NH$_3$:1 CO	
Amide III (primary)	1409	1408	1409	. . .	. . .	1420–1400
Amine NH bending	1640	1647	1587	1602	1603	1650–1580
Amide I	1684	1691	1686	1682	1680	1680–1630
NH$_4$$^+$ OCN$^-$ (NH stretching)	3032	2973	2824	2960	. . .	?
Amine NH stretching	3303	3315	3284	3297	3340	3500–3300

however, as our study was in bulk and not matrix isolated, we cannot compare the peaks directly). Unfortunately, the v_1 and v_2 bands overlap with the spectral features of the pristine ice, e.g., broad ammonia peak from 3200 to 3500 cm^{-1} and are in close proximity to products identified after irradiation, e.g., OCN^{-1} at 2157 cm^{-1}. The weaker bands, v_3 and v_5, were also

not observed. Accordingly, we may state that no direct evidence was available elucidating the appearance of isocyanic acid.

3.2. Mass Spectrometry

In all experiments no observable signal was detected above background levels during irradiation, including molecular

Table 7
Reaction Rate Constants Derived from Fitting the Column Density of the Respective Molecule with the Particular Model as Listed

Molecule	Model	11 CO:2 NH$_3$	5 CO:2 NH$_3$	2 CO:5 NH$_3$ k (s^{-1})	10 NH$_3$:1 CO	20 NH$_3$:1 CO
CO	$[CO]_{t=0}\left(e^{-kt}\right)$	$1.2 \pm 0.9 \times 10^{-5}$	$2.8 \pm 0.5 \times 10^{-5}$	$1.2 \pm 0.5 \times 10^{-3}$	$7.2 \pm 0.4 \times 10^{-5}$	$9.0 \pm 0.6 \times 10^{-5}$
NH$_3$	$[NH_3]_{t=0}\left(e^{-kt}\right)$	$1.8 \pm 0.1 \times 10^{-4}$	$9.2 \pm 0.7 \times 10^{-3}$	$4.7 \pm 1.1 \times 10^{-5}$	$1.7 \pm 0.2 \times 10^{-5}$	$1.5 \pm 0.2 \times 10^{-5}$
HCO	$a\left(1 - e^{-kt}\right)$	$5.2 \pm 3.1 \times 10^{-4}$	$4.2 \pm 1.4 \times 10^{-4}$	–	–	–
H$_2$NCHO	$a\left(1 - e^{-kt}\right)$	$5.4 \pm 1.0 \times 10^{-4}$	$5.1 \pm 1.2 \times 10^{-4}$	$3.3 \pm 1.0 \times 10^{-4}$	$5.2 \pm 1.1 \times 10^{-4}$	$5.0 \pm 1.3 \times 10^{-4}$

hydrogen, contrasting that which has been previously seen during the irradiation of pure methane (Bennett et al. 2006), and a binary mixture of carbon monoxide–methane ices (Bennett et al. 2005). As the sample was warmed to a temperature of 240 K, a signal appeared at $m/z = 45$ and 43, corresponding to the parent ion of formamide (H$_2$NCHO$^+$) and the fragment of formamide (NCOH$^+$). However, it should be pointed out that this signal was distinguishable only for the irradiated 5:2 ice matrix. The lack of detectable signal during the sublimation phase suggests formamide undergoing polymerization and/or perhaps further reactions with other molecular species present as it is heated, leading to the synthesis of the larger more complex organics. This agrees with previous results that formamide was not detected via subsequent mass spectrometry analysis on the residue formed as well as the observation that IR bands of formamide disappeared at a temperature of approximately 270 K (Grim et al. 1989).

4. DISCUSSION

Having identified the formamide molecule in the electron-irradiated carbon monoxide–ammonia ices, the temporal evolution of the observed column densities of formamide and its precursor molecules may now be plotted and fitted kinetically during the irradiation of the ice samples. Recall that the proposed reaction scheme is summarized in reactions (1)–(3) above. However, we have already discounted the possibility of reaction scheme (1) occurring. At this point, it should be reiterated that no clear evidence of the NH$_2$CO radical or HNCO was witnessed in the irradiation experiments. Our results suggest rather that the initial step in the synthesis of formamide is the unimolecular decomposition of the ammonia molecule (internal energy is incorporated into the ammonia molecules from the energetic electrons) via cleavage of a nitrogen–hydrogen bond to generate the amino radical and atomic hydrogen. As pointed out above, this reaction is endoergic by 435 kJ mol^{-1}. Considering a unimolecular decomposition of ammonia and hence a first-order decay, the temporal profile of ammonia was fitted using a first-order decay rate law as follows:

$$[NH_3]_t = [NH_3]_{t=0}\, e^{-k_1 t}.$$

The temporal evolution of the column density for the destruction of ammonia and thus the production of atomic hydrogen was determined from the v_2 band at $\sim$1070 cm^{-1} and the broadband ranging from 3200 to 3500 cm^{-1} using the A values as listed in Table 2. The reaction rate constant (k_1) for the unimolecular decay of ammonia for each irradiated ice sample is summarized in Table 7. Note that this process also releases energetic hydrogen atoms with an excess energy of a few hundred kJ mol^{-1} (Bennett et al. 2006). These suprathermal hydrogen atoms may then add to the carbon–oxygen triple bond of carbon monoxide forming the formyl radical (HCO), reaction scheme (3b). Experimental investigations have shown this reaction to

be exoergic by 60–70 kJ mol^{-1} (Smith et al. 1991; Wang et al. 1973; Werner et al. 1995) while a theoretical treatment of the hydrogen addition to carbon monoxide using density functional theory at the B3LYP, B3P86, and B3PW91 levels (Jursic 1998) along with CCSD(T) calculation (Bennett et al. 2005) yielded a value similar to the experimental in conjunction with an energy barrier of 10.5–11.2 kJ mol^{-1} matching well with the experimentally derived activation barrier of 8.4 ± 1.4 kJ mol^{-1} (Wang et al. 1973). The energy necessary to overcome this barrier is easily supplied by the excess kinetic energy of the hydrogen atom produced in the destruction of ammonia. In the kinetic model, we propose that the rate of formation of the formyl radical should be related to the suprathermal hydrogen atoms via a pseudo-first-order rate:

$$[HCO]_t = a_1(1 - e^{-k_2 t}).$$

For the formyl radical, we used the v_3 (CO stretching) absorption at 1857 cm^{-1} and 1855 cm^{-1} identified in the 11:2 and 5:2 ices, respectively, using an A value of 1.5×10^{17} (Bennett et al. 2005). Fitting the temporal evolution of the determined column density for HCO yielded a k value of $5.2 \pm 3.1 \times 10^{-4}$ s^{-1} for the 11:2 ice and $4.2 \pm 1.4 \times 10^{-4}$ s^{-1} for the 5:2 irradiated ice (Table 7). As mentioned previously, the formyl radical was not observed for the 2:5, 1:10, or the 1:20 (CO:NH$_3$) irradiated ices. This observation may be rationalized as such: the observed HCO radical is the excess which has not reacted and that as the concentration of carbon monoxide decreases, the amount of formyl radical will also decrease and consequently will be below the detectable limit of the experimental setup.

Alternatively, the reaction may proceed through an intermediate step involving the carbamyl (NH$_2$CO) radical (reaction scheme (2)). This requires first the destruction of ammonia followed with the amino radical reacting with carbon monoxide; unfortunately no empirical evidence of the carbamyl radical was seen. A theoretical investigation has shown this reaction to have a reaction energy barrier of 15 kJ mol^{-1} with an overall reaction exogercity of 75 kJ mol^{-1} (Zhang et al. 2004). From this point, atomic hydrogen may add to the carbamyl radical, concluding the reaction with the formation of formamide (scheme (2c)) or it may undergo a reaction with itself (disproportionate), forming isocyanic acid in addition to formamide (reaction scheme (2d)). A gas-phase study determined the disproportionate reaction to have an activation energy of $\sim$146 kJ mol^{-1} (Yokota & Back 1973) which is significantly less than the excess energy gained from the previous step (2b) and so is unlikely to occur. We should also mention that a recent investigation on the formation mechanism of OCN$^-$ has determined that this molecular species is formed through a spontaneous reaction of isocyanic acid (HNCO) with ammonia. Since OCN$^-$ has been observed both in the experiment and in multiple previous experiments (Demyk et al. 1998; Hagen 1982; Hudson & Moore 2000; Raunier et al. 2003), we may conclude that HNCO is formed albeit from a different pathway (Bennett et al. 2010).
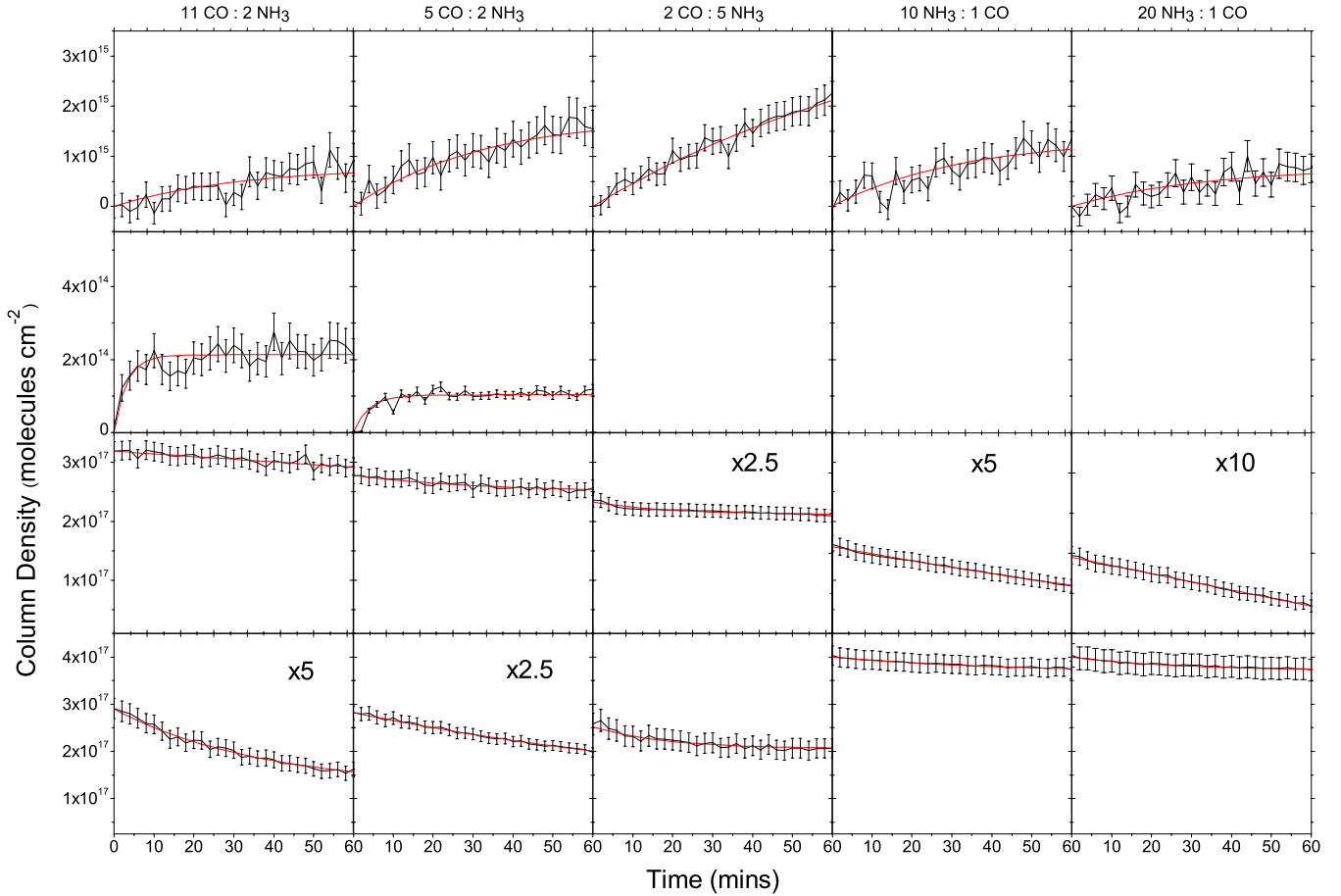
Figure 2. Temporal profiles of the column densities for the respective molecule (as pictured) during irradiation. Experimental data along with the error bars are shown in black along with the kinetic fits (red). The kinetic models are stated in the main text and Table 7. Carbon monoxide and ammonia were multiplied by a factor (shown) in order to maintain a common scale for both species. Here the figure is oriented such that the respective concentration of carbon monoxide decreases from left to right.

(A color version of this figure is available in the online journal.)

The loss of carbon monoxide involves only one step in all of the above mentioned reaction pathways. Consequently, the kinetic fitting should reflect a first-order rate law. The decay profile for carbon monoxide was fitted using a first-order decay similar to that of ammonia:

$$[CO]_t = [CO]_{t=0}\, e^{-k_3 t}.$$

The kinetic rate constants (k) are listed in Table 7 for the temporal evolution of the carbon monoxide column densities.

If the formyl radical and the amino radical are generated inside the matrix cage and also hold the correct geometry, then they can recombine without an energy barrier to form formamide via reaction scheme (3c). If the recombination geometry is not reached or if the radicals are not generated in close proximity, these radicals will remain isolated within the carbon–ammonia ice and will not combine. Note that the reaction exoergicity is 420 kJ mol^{-1} based on the NIST database values (Afeefy et al. 2010). To fit the data in our experiments we suggest that the first step involves the pseudo-first-order generation of the amino and formyl radicals in a matrix cage generated in the right orientation to recombine without an energy barrier in a second reaction step leading to formamide. This process should adhere to a consecutive pathway as follows:

$$[CO...NH_3] \xrightarrow{k_1} [HCO...NH_2] \xrightarrow{k_2} [H_2NCOH]\,,$$

where the concentration of formamide should follow a sequential reaction with two steps as dictated by the following equation:

$$[H_2NCOH]_t = a\left(1 - \frac{k_2}{k_2 - k_1}e^{-k_1 t} + \frac{k_1}{k_2 - k_1}e^{-k_2 t}\right);$$

however, in the event that $k_2 \gg k_1$ this equation can be simplified to a pseudo-first-order model:

$$[H_2NCOH]_t = a(1 - e^{-k_1 t}).$$

As mentioned before, the column density of formamide was measured using the ν_6 (CH scissoring) band at 1389 cm^{-1} using the experimentally derived A constant of 6.8×10^{-16} cm mol^{-1} (Brucato et al. 2006a) as this band was the only one isolated enough to integrate without involving a deconvolution technique. Fitting our data to the above equation yielded reaction rate values for each irradiated ice, all within the range of 3–5 $\times$ 10^{-4} s^{-1}; for details see Table 7. The kinetic models for the temporal evolution of the column densities for carbon monoxide (CO), ammonia (NH$_3$), hydroxyl radical (HCO), and formamide (H$_2$NCHO) are shown in Figure 2 for each of the irradiated ice mixtures.

The reaction kinetics of this system may be compared to that of a similar system in which the HCO radical was identified as an intermediate step. It was also shown in a previous study on the formation of acetaldehyde upon the electron irradiation of a
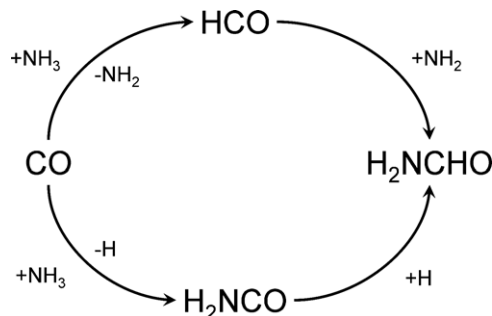
Figure 3. Summary of the reaction pathways leading to the production of formamide (H_2NCHO) in carbon monoxide–ammonia ices undergoing energetic processing. As mentioned in the text, no experimental evidence was found for the carbamyl radical (H_2NCO) due to the overlapping features in the IR spectra. Consequently, this is a suggested pathway.

Table 8
Percent Yield of Formamide Produced After 60 minutes of Irradiation
Relative to the Limiting Reagent

Ice Ratio (X CO:Y NH$_3$)	Percent Yield
11:2	1.1 ± 0.3
5:2	1.8 ± 0.3
2:5	2.4 ± 0.7
1:10	2.6 ± 0.6
1:20	3.6 ± 0.7

binary mixture containing methane (CH_4) and carbon monoxide (CO). The temporal profile of the HCO column density was kinetically found to be a pseudo-first-order reaction similar to this experiment; however, the k value was determined to be an order of magnitude faster at $3.8 \pm 0.6 \times 10^{-3}$ s^{-1}. The discrepancy may be resolved in the physical differences between the two binary ice matrices. Although both methane and ammonia have similar bond energies, hydrogen bond rupture of methane may be more prevalent in the CO/CH$_4$ ice than in the CO/NH$_3$ one as the energy maybe dispersed more efficiently in the lattice modes of the latter. The fraction of kinetic energy of each impinging electron in the previous experiment involving the electron bombardment of a CO/CH$_4$ ice matrix was determined to be 2.5% (Bennett et al. 2005). Following the same argument, we may calculate the fraction of kinetic energy that was partitioned into the 11:2 and 5:2 ice matrices. Although the amino radical was not directly observed, we may assume the total concentration of the amino radical to be simply the difference in the initial ammonia concentration $[NH_3]_{t=0}$ and that after the total electron exposure time $[NH_3]_{t=60}$ as per reaction steps (2a) and (3a) while neglecting other destructive pathways. Consequently, this assumption will produce an upper limit as to the amount of amino radical produced and thus the maximum percentage of kinetic energy partitioned from the impinging electron. For the 11:2 ice, the maximum amount of NH$_2$ radical formed is $2.6 \pm 0.3 \times 10^{16}$ and $3.2 \pm 0.4 \times 10^{16}$ molecules cm^{-2} for the 5:2 ice. Taking into account the total number of electrons (1.8×10^{15}), each electron would then generate 14 ± 2 amino radicals in the 11:2 ice and 18 ± 2 amino radicals in the 5:2 ice. Considering the N–H bond energy of 435 kJ mol^{-1} (4.5 eV) for ammonia, an energy transfer of 63 and 81 eV, respectively, for the 11:2 and 5:2 ices is necessary to account for the amount of NH$_2$ proposed. This would correspond to a maximum amount of 1.2%–1.6% of the kinetic energy of each impinging electron used in the formation of the amino radical as the electron is being absorbed in the sample and 5 keV electrons are available. This value is approximately one-half to two-thirds of that determined in the CO/CH$_4$ ice which would suggest that the excess energy is dispersed more efficiently in the lattice modes of the CO/NH$_3$ ice matrices as compared to the CO/CH$_4$ ice, and consequently a slower rate in the production of formyl (HCO) radical.

The overall net reaction is reflected in reaction scheme (1), with the proposed reaction pathways summarized in Figure 3. Here the maximum amount of formamide produced is constrained by the limiting reagent. Accordingly, we may calcu-

late the percent yield as simply the ratio between amount of formamide produced after irradiation to that of the initial concentration of the limiting reagent, i.e., ammonia for the carbon-monoxide-rich ices and carbon monoxide in the ammonia-rich ices. The results of this are summarized in Table 8. The percent yield increased rather linearly as a function of ammonia present. The lowest yield was the 11:2 ice with a value of $1.1\% \pm 0.3\%$ relative to ammonia while the highest percent was $3.6\% \pm 0.6\%$ relative to the limiting reagent of carbon monoxide within the 1:20 irradiated ice sample. This result agrees well with the implication that the initial step toward the synthesis of formamide is the bond rupture of ammonia, i.e., the more ammonia present, the more it will undergo hydrogen bond rupture producing higher concentrations of NH$_2$ and hydrogen atom to react with carbon monoxide.

For each of the irradiated ice matrices, a residue was formed upon heating the sample to a final temperature of 300 K. An IR spectrum of the residue was taken before and after venting the main chamber with no considerable changes witnessed, suggesting that the residue is stable toward oxidation and hydrolysis from the water in air. The residue of each irradiated ice sample is shown on the right-hand side of Figure 1 (black line) along with a Gaussian deconvolution (red line) of the observed peaks. What appeared to be unassigned peaks are the result of a change in the background and consequently are irrelevant to the experiment. Grim et al. identified several different compounds within the residue formed from the photolysis of a binary CO/NH$_3$ mixture at 10 K including urea (H_2NCONH_2), oxamide ($H_2NCOCONH_2$), and buiret ($H_2NCONHCONH_2$) (Grim et al. 1989). In addition to these molecules, Agarwal et al. (1985) found biurea ($H_2NCO(NH_2)_2CONH_2$), oxamic acid ($H_2NCOCOOH$), lactic acid ($H_3CCH(OH)CO_2H$), glycolic acid ($HOCH_2CO_2H$), hydroxyl acetamide ($HOCH_2CONH_2$), glyceric acid ($HOCH_2CH(OH)CO_2H$), and glyceramide ($HOCH_2CH(OH)CONH_2$). However, a direct comparison of these two studies is not valid as the experimental technique used in the study presented by Agarwal involved exposing the CO/NH$_3$ gas mixture to high-energy photons while condensing onto an aluminum surface held at 10 K, and thus consisted primarily of gas-phase reactions. The residue observed within the presented studies should be similar to that of Grim et al. where oxamide was proposed to be the product of a carbamyl radical self-reaction. Formation of biuret involves a slightly more complicated process. Here, imidogen (NH; formed during the destruction of ammonia) may react with the carbamyl radical leading to the H_2NCONH radical whereupon it can proceed to react with another carbamyl radical, concluding with the formation of biuret. The lack of evidence of formamide sublimating in the gas phase (save for the 5:2 irradiate ice sample) suggests that formamide may undergo polymerization or further reactions with any of the several compounds mentioned above while heating after the carbon monoxide and ammonia have sublimated.

Based on previous experiments identifying the molecular composition of the residue and the hypothesis of formamide proceeding through additional reactions, we may tentatively assign the observed IR peaks with characteristic active modes, as summarized in Table 6. The strongest peak observed was characterized as an amide I bond which results from the C–O stretching coupled with the N–H bending and C–N stretching observed from 1680 to 1690 cm^{-1}. The peak intensity of this band correlated exponentially with the relative amount carbon monoxide present in the pristine ice sample, except for the 5:2 irradiated ice; connecting well with the mass spectrum observation of formamide sublimating into the gas phase for this particular irradiated ice ratio. A very broad peak with slightly less intensity was observed in the vicinity of 3500–2500 cm^{-1}. This peak was deconvoluted with the minimum number of Gaussian functions leading to an acceptable fit yielding two peaks centered at approximately 3000 and 3300 cm^{-1} for each of the residues, which are typical wavenumbers for N–H stretching. Given the molecules identified in the residues of previous experiments, it is understandable why this peak would be so broad and featureless. Two smaller peaks were identified and tentatively characterized as NH_2 bending at IR wavenumbers of $\sim$1600 cm^{-1} and a primary amide (III) bond with typically observable IR frequencies in the range of 1420–1400 cm^{-1}.

5. ASTROPHYSICAL IMPLICATIONS

The present study demonstrates that the formation of formamide in binary icy mixtures of carbon monoxide and ammonia is possible when subjected to irradiation by energetic particles such as electrons. Similar processes can occur within the icy grains of the interstellar medium and have been demonstrated experimentally from VUV/UV photon irradiation (Demyk et al. 1998; Ferris et al. 1974; Grim et al. 1989; Hudson & Moore 2000; Milligan & Jacox 1965) and MeV protons (Hudson & Moore 2000), the latter of which is responsible for the transfer of energy into the electronic systems of a molecular species trapped in an icy matrix. Our study has shown for the first time that the production of the formyl radical is definitive within the carbon-monoxide-rich ices and is consequently a plausible outcome even in the ammonia-rich ices. The process is initiated by nitrogen–hydrogen bond rupture in the ammonia molecule to form the amino radical and a hydrogen atom of which holds an excess of kinetic energy and thus is not in thermoequilibrium with the surrounding cold (12 K) matrix. The excess kinetic energy of the hydrogen atom can be dispersed into the transition state with the addition of a hydrogen atom to the carbon monoxide molecule, leading to the formation of the formyl radical (HCO) easily overcoming the barrier of this reaction at 8.4 ± 1.4 kJ mol^{-1} (Jursic 1998). If the formyl radical and the amino radical have the correct orientation within the matrix, both species can undergo a barrierless radical–radical combination within the matrix cage to synthesize formamide. Although the carbamyl radical (H_2NCO) was not identified in the current study, we cannot rule out the possibility of this species being present as the strongest IR-active modes being indistinguishable from the precursors as well as the other products identified. Here the amino radical formed from the initial dissociation of the ammonia molecule can add to the triple bond of carbon monoxide as well. The barrier for the reaction as mentioned above was determined to be 15 kJ mol^{-1} (Zhang et al. 2004). However, the amino radical can be formed with internal excitation (rovibrational or electronic) as all of the excess energy is not partitioned into the translational energy

of the hydrogen atom and consequently has the capability to overcome the reaction barrier to form the carbamyl radical. In a similar fashion to the reaction of HCO with NH_2, the carbamyl radical and hydrogen atom may undergo a barrierless reaction if both species are present within the matrix along with the proper geometric orientation ultimately ending with the production of formamide. In summary, the most realistic reaction pathways (reaction schemes (2a)–(2c) and (3)) leading to the production of formamide are shown in Figure 3.

This experiment simulates the typical time of a molecular cloud during which the pristine icy mantles of grains are subjected to background cosmic-ray radiation leading to the formation of more complex molecules. Typically, an explanation as to how the newly synthesized molecules within the icy grain mantle resulting from the energetic processing end up in gas phase is that the grains are subjected to thermal radiation via the beginning stages of star birth near the center of the molecular cloud at which point the molecules will begin to sublimate slowly into the gas phase and continue to do so as the temperature increases. Our results would suggest that this mechanism can only be partially responsible for the presence of formamide in the gas phase. This is evident in the lack of detectable signal in the mass spectrometer and the trend of the amide I bond peak intensity identified to have an exponential growth as a function of the $CO:NH_3$ ratio, with the exception of the 5:2 irradiate ice. Instead, the observation of gas-phase formamide within Sgr B2(N) would be more likely explained through grain–grain collisions and/or through shocking of the interstellar medium (Flower & Pineau des Forets 1994). Similarly, the observation of acetamide in Sgr B2(N) (Hollis et al. 2006) may be explained by the energetic processing of an icy mantle containing methane in addition to ammonia and carbon monoxide or water. This suggestion may be validated as acetamide has already been shown to be a product of the result of high-energy proton irradiation ices containing a ternary mixture of methane, water, and ammonia at 77 K (Berger 1961).

To paraphrase, the presence of formamide within the interstellar medium is suggested to be the result from the energetic processing of icy grains. In order for the previous statement to be correct, empirical evidence must validate the suggestion that carbon monoxide and ammonia would neighbor each other in an icy grain mantle within the interstellar medium. Indeed, as shown in a thorough study by Gibb et al. (2004) of 23 infrared sources utilizing the *Infrared Space Observatory* (*ISO*), they were able to confirm in 13 of these sources the presence of carbon monoxide and ammonia existing within the icy grain mantle of these young stellar objects (YSOs). Furthermore, of the YSOs surveyed, two have these which have already had formamide tentatively assigned including high-mass YSO NGC 7538 IRS9 (Raunier et al. 2004) and W33A (Schutte et al. 1999). YSO NGC 7538 IRS9 has a CO abundance of 17% with an ammonia abundance of 15% relative to water and has been labeled as a YSO undergoing weak energetic processing, where as the YSO W33A (labeled as undergoing strong processing) was found to have a CO abundance of 8.2% with an NH_3 abundance <15% (Gibb et al. 2004). Given the assignment of formamide within these YSOs, and the experimental evidence that formamide is formed during the energetic processing of a carbon-monoxide–ammonia ice, we may suggest the presence of formamide among the several other objects undergoing energetic processing identified by Gibb et al. as well as other unknown objects throughout the interstellar medium indentified to be carriers of both carbon monoxide and ammonia. Furthermore, the residue resulting from the

energetic processing of such ices may hold relevance to prebiotic chemistry. A common perception is that the organic materials necessary for the development of the probiotic chemical framework are that these compounds accumulated onto an early earthlike environment from the deposition of interstellar dust, comets, and meteorites (Brack 1999; Walker 1977). The results of this and previous experiments establish this assumption to be a significant possibility, as the energetic processing of even a simple binary ice mixture of carbon monoxide and ammonia leads to a non-volatile and stable residue consisting primarily of urea, oxamide, and biuret, all of which are molecules containing the biologically important peptide bond.

REFERENCES

Afeefy, H. Y., Liebman, J. F., & Stein, S. E. 2010, in Neutral Thermochemical Data, ed. P. J. Linstrom & W. G. Mallard (Gaithersburg, MD: National Institute of Standards and Technology)
Agarwal, V. K., Schutte, W., Greenberg, J. M., Ferris, J. P., Briggs, R., Connor, S., Van de Bult, C. P. E. M., & Baas, F. 1985, Orig. Life Evol. Biosph., 16, 21
Apene, I., & Mikstais, U. 1978, Khimiko–Farmatsevticheskii Zh., 12, 84
Bennett, C. J., Jamieson, C., Mebel, A. M., & Kaiser, R. I. 2004, Phys. Chem. Chem. Phys., 6, 735
Bennett, C. J., Jamieson, C. S., Osamura, Y., & Kaiser, R. I. 2005, ApJ, 624, 1097
Bennett, C. J., Jones, B., Knox, J. E., Perry, J., Kim, Y. S., & Kaiser, R. I. 2010, ApJ, 723, 641
Bennett, C. J., & Kaiser, R. I. 2007, ApJ, 660, 1289
Bennett, C. J., Jamieson, C. S., Osamura, Y., & Kaiser, R. I. 2006, ApJ, 653, 792
Berger, R. 1961, Proc. Natl. Acad. Sci. USA, 47, 1434
Bockelée-Morvan, D., et al. 2000, A&A, 353, 1101
Boden, J. C., & Back, R. A. 1970, Trans. Faraday Soc., 66, 175
Brack, A. 1999, Adv. Space Res., 24, 417
Broekhuizen, F. A., Keane, J. V., & Schutte, W. A. 2004, A&A, 415, 425
Brucato, J. R., Baratta, G. A., & Strazzulla, G. 2006a, A&A, 455, 395
Brucato, J. R., Strazzulla, G., Baratta, G. A., Rotundi, A., & Colangeli, L. 2006b, Orig. Life Evol. Biosph., 36, 451
Bujdák, J., & Rode, B. M. 1999, Orig. Life Evol. Biosph., 29, 451
Costanzo, G., Saladino, R., Crestini, C., Ciciriello, F., & Di Mauro, E. 2007, BMC Evol. Biol., 7, S1
Dederichs, B., & Saus, A. 1977, Radiation Phys. Chem., 10, 227
Demyk, K., Dartois, E., & d'Hendecourt, L. 1998, A&A, 339, 553
d'Hendecourt, L. B., & Allamandola, L. J. 1986, A&AS, 64, 453
Ewing, G. E., Thompson, W. E., & Pimentel, G. C. 1960, J. Chem. Phys., 32, 927
Ferris, J. P., Williams, E. A., Nicodem, D. E., Hubbard, J. S., & Voecks, G. E. 1974, Nature, 249, 437
Flower, D. R., & Pineau des Forets, G. 1994, MNRAS, 268, 724
Forney, D., Jacox, M. E., & Thompson, W. E. 2003, J. Chem. Phys., 119, 10814
Gerakines, P. A., Schutte, W. A., Greenberg, J. M., & Van Dishoeck, E. F. 1995, A&A, 296, 810
Gerakines, P. A., Bray, J. J., Davis, A., & Richey, C. R. 2005, ApJ, 620, 1140
Gerakines, P. A., Moore, M. H., & Hudson, R. L. 2001, J. Geophys. Res., 106, 33381
Gibb, E. L., Whittet, D. C. B., Boogert, A. C. A., & Tielens, A. G. G. M. 2004, ApJS, 151, 35
Grim, R. J. A., Greenberg, J. M., DeGroot, M. S., Baas, F., Schutte, W. A., & Schmitt, B. 1989, A&AS, 78, 161
Hagen, W. 1982, Ph.D. thesis, Univ. of Leiden

Harvey, K. B., & Ogilvie, J. F. 1962, Can. J. Chem., 40, 85
Hollis, J. M., Lovas, F. J., Remijan, A. J., Jewell, P. R., Ilyushin, V. V., & Kleiner, I. 2006, ApJ, 643, L25
Hovington, P., Drouin, D., & Gauvin, R. 1997, Scanning, 19, 1
Hubbard, J. S., Voecks, G. E., Hobby, G. L., Ferris, J. P., Williams, E. A., & Nicodem, D. E. 1975, J. Mol. Evol., 5, 223
Hudgins, D. M., Sandford, S. A., Allamandola, L. J., & Tielens, A. G. G. M. 1993, ApJS, 86, 713
Hudson, R. L., & Moore, M. H. 2000, A&A, 357, 787
Ivanov, C., & Vladovska, Y. 1978, Dokl. Bolgarskoi Akad. Nauk, 31, 1605
Jacox, M. E. 1988, J. Chem. Phys., 88, 4598
Jacox, M. E., & Milligan, D. E. 1963, Spectrochim. Acta, 10, 1173
Jamieson, C. S., Mebel, A. M., & Kaiser, R. I. 2006, ApJS, 163, 184
Johnson, R. E. 1990, Energetic Charged-Particle Interactions with Atmospheres and Surfaces, Vol. 19 (New York: Springer)
Jursic, B. S. 1998, J. Mol. Struct., 427, 157
Kaiser, R. I. 2002, Chem. Rev., 102, 1309
Kaiser, R. I., & Roessler, K. 1998, ApJ, 503, 959
Kakumoto, T., Saito, K., & Imamura, A. 1985, J. Phys. Chem., 89, 2286
Kim, K., Lee, B., & Lee, S. 1998, Bull. Korean Chem. Soc., 19, 553
King, S.-T. 1971, J. Phys. Chem, 75, 405
Kostakis, I. K., Elomri, A., Seguin, E., Iannelli, M., & Besson, T. 2007, Tetrahedron Lett., 48, 6609
Krupskii, I. N., Prokhvatilov, A. I., Erenburg, A. I., & Yantsevich, L. D. 1973, Phys. Status Solidi a, 19, 519
Lambert, J.-F. 2008, Orig. Life Evol. Biosph., 38, 211
Lambert, J.-F., Stievano, L., Lopes, I., Gharsallah, M., & Piao, L. 2009, Planet. Space Sci., 57, 460
Maier, G., & Lautz, C. 1998, Eur. J. Org. Chem., 1998, 769
Markwick, A. J., Millar, T. J., & Charnley, S. B. 2000, ApJ, 535, 256
Milligan, D. E., & Jacox, M. E. 1965, J. Chem. Phys., 43, 4487
Milligan, D. E., & Jacox, M. E. 1969, J. Chem. Phys., 51, 277
Milligan, D. E., & Jacox, M. E. 1971, J. Chem. Phys., 54, 927
Minkwitz, R. Z. 1975, Anorg. Allg. Chem., 1, 411
Nguyen, V. S., Abbott, H. L., Dawley, M. M., Orlando, T. M., & Leszczynski, J. 2011, J. Phys. Chem A, 115, 841
Pettersson, M., Khriachtchev, L., Jolkkonen, S., & Rasanen, M. 1999, J. Phys. Chem A, 103, 9154
Raunier, S., Chiavassa, T., Duvernay, F., Borget, F., Aycard, J. P., Dartois, E., & d'Hendecourt, L. 2004, A&A, 416, 165
Raunier, S., Chiavassa, T., Marinelli, F., Allouche, A., & Aycard, J. P. 2003, Chem. Phys. Lett., 368, 594
Rimola, A., Tosoni, S., Sodupe, M., & Ugliengo, P. 2006, ChemPhysChem, 7, 157
Romanescu, C., Marschall, J., Kim, D., Khatiwada, A., & Kalogerakis, K. S. 2010, Icarus, 205, 695
Rubin, R. H., Swenson, G. W., Beson, R. C., Tigelaar, H. L., & Flygare, W. H. 1971, ApJ, 169, L39
Saladino, R., Ciambecchini, U., Crestini, C., Costanzo, G., Negri, R., & Mauro, E. D. 2003, ChemBioChem, 4, 514
Saladino, R., Crestini, C., Ciciriello, F., Costanzo, G., & Di Mauro, E. 2007, Chem. Biodiversity, 4, 694
Saladino, R., Crestini, C., Ciciriello, F., Pino, S., Costanzo, G., & Di Mauro, E. 2009, Res. Microbiol., 160, 441
Saladino, R., Crestini, C., Costanzo, G., Negri, R., & Di Mauro, E. 2001, Bioorg. Med. Chem., 9, 1249
Saladino, R., Crestini, C., Neri, V., Brucato, J. R., Colangeli, L., Ciciriello, F., Di Mauro, E., & Costanzo, G. 2005, ChemBioChem, 6, 1368
Schutte, W. A., et al. 1999, A&A, 343, 966
Scoville, N. Z., Solomon, P. M., & Penzias, A. A. 1975, ApJ, 201, 352
Senanayake, S. D., & Idriss, H. 2006, Proc. Natl. Acad. Sci. USA, 103, 1194
Smith, B. J., Nguyen Minh, T., Bouma, W. J., & Radom, L. 1991, J. Am. Chem. Soc., 113, 6452
Suzer, S., & Andrews, L. 1987, J. Phys. Chem., 87, 5131
Sylwester, A. P., & Dervan, P. B. 1984, J. Am. Chem. Soc., 106, 4648
Walker, J. C. G. 1977, Evolution of the Atmosphere (New York: MacMillan)
Wang, H. Y., Eyre, J. A., & Dorfman, L. M. 1973, J. Chem. Phys., 59, 5199
Werner, H.-J., Bauer, C., Rosmus, P., Keller, H.-M., Stumpf, M., & Schinke, R. 1995, J. Chem. Phys., 102, 3593
Woolley, W. D., & Back, R. A. 1968, Can. J. Chem., 46, 295
Yamada, H., & Person, W. B. 1964, J. Chem. Phys., 41, 2478
Yokota, T., & Back, R. A. 1973, Int. J. Chem. Kinetics, 5, 37
Zhang, W., Du, B., & Feng, C. 2004, J. Mol. Struct., 679, 121
Zheng, W., Jewitt, D., Osamura, Y., & Kaiser, R. I. 2008, ApJ, 674, 1242
Zheng, W., & Kaiser, R. I. 2007, Chem. Phys. Lett., 440, 229